molecular pharmaceutics

Article

pubs.acs.org/molecularpharmaceutics

Flash Nanoprecipitation: Prediction and Enhancement of Particle Stability via Drug Structure

Zhengxi Zhu*

Department of Chemical Engineering and Materials Science, University of Minnesota, Minneapolis, Minnesota 55455, United States

Supporting Information

ABSTRACT: Flash nanoprecipitation (FNP) can generate hydrophobic drug nanoparticles in ~100 nm with a much higher drug loading (e.g., > 40 wt %) than traditional nanocarriers (e.g., < 20 wt %). This paper studies the effects of drug molecules on nanoparticle stability made via FNP and demonstrates that chemically bonding a drug compound (e.g., paclitaxel) with a cleavable hydrophobic moiety of organosilicate (e.g., triethoxysilicate) is able to enhance the particle size stability. A nonionic amphiphilic diblock copolymer, poly(lactic-*co*-glycolic acid)-*block*-poly(ethylene glycol) (PLGA-*b*-PEG), is used as a model surfactant to provide steric stabilization. The experiments here show that the lower the drug solubility in the aqueous medium, the more stable the particles in terms of Ostwald ripening, which are consistent with the prediction by the LSW theory. The initial particle size distribution is sufficiently narrow and of insignificance to Ostwald ripening. To correlate the particle stability with hydrophobicity, this study introduces the *n*-octanol/water partition coefficient (Log*P*), a hydrophobicity indication, into the FNP technique. A comparison of various drugs and their analogues shows that Log*P* of a drug is a better hydrophobicity indication than the solubility parameter (δ) and correlates well with the particle stability. Empirically, with ACDLog*P* > ~12, nanoparticles have good stability; with ~2 < ACDLog*P* < ~9, nanoparticles show fast Ostwald ripening and interparticle recrystallization; with ACDLog*P* < ~2, the drug is very likely difficult to form nanoparticles. This rule creates a quick way to predict particle stability for a randomly selected drug structure and helps to enable a fast preclinical drug screen.

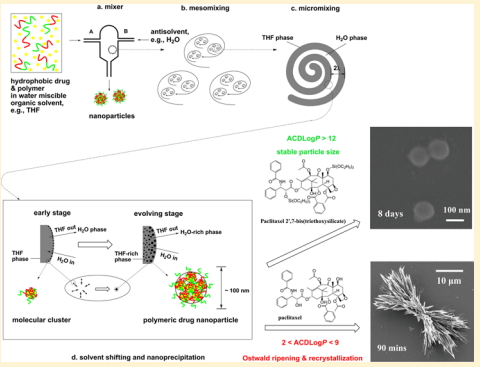

KEYWORDS: *drug delivery, NCI drug dictionary, flash nanoprecipitation, nanoparticle stability, paclitaxel organosilicate prodrug, block copolymer, preclinical drug screen, LogP*

INTRODUCTION

At least 30−40% of new drug candidates have poor water solubility and are difficult to be administrated.[1] However, the trend of drug discovery is toward more hydrophobicity and thus better permeability to get through the gastrointestinal tract wall and cell membranes.[1] An enhanced dissolution rate is able to compensate for the poor solubility. A variety of nanoscaled particles as carriers therefore have been engineered, since they have much higher surface areas and thus dissolution rates.[2] Moreover, particles in the size range of about 50−400 nm are able to accumulate in tumors during in vivo blood circulation due to the enhanced permeability and retention (EPR) effect.[3] This passive targeting can enhance efficacy and reduce chemotherapy side effects. Compared with different nanoscaled particles, i.e., micelles,[4−7] liposomes,[8] and nanoemulsions[9,10] with a typical drug loading capacity (C_{DL} %) below 20%, nanosuspensions[11−14] (usually called nanoparticles) have a much higher drug loading and are able to show sufficient potency to kill tumors.

Among different techniques to produce nanoparticles, i.e., milling, high pressure homogenization, and the supercritical fluid process, flash nanoprecipitation (FNP) shows advantages of fast processing, simple equipment, smaller size, and narrower size distribution.[15−24] The FNP also permits combining several hydrophobic drugs and the incorporation of imaging agents.[25] In the FNP technique[18] (see Figure 1), a highly hydrophobic drug is dissolved along with a block copolymer (BCP) in a water miscible organic solvent. This solution is injected into a small chamber at a high velocity along with water. The high velocity generates turbulent mixing, causing the hydrophobic drug and polymer to coprecipitate very rapidly, forming nanoscaled particles. The block copolymer is amphiphilic: typically a hydrophilic poly(ethylene glycol) (PEG) block covalently bonded to a hydrophobic block. The hydrophobic block precipitates with the drug, arresting particle growth, while the pendant PEG blocks stabilize the particles against aggregation.[23]

However, like many other techniques, the challenge of particle stability still exists. In our previous work, various polymers as the stabilizers, i.e., water-soluble polyelectrolytes (polylysine, polyethylene imine, and chitosan)[23] and nonionic amphiphilic diblock copolymers [polystyrene-*block*-poly(ethylene glycol) (PS-*b*-PEG), polycaprolactone-*block*-poly(ethylene glycol) (PCL-*b*-PEG), polylactide-*block*-poly-

Received: August 12, 2013
Accepted: February 3, 2014
Published: February 3, 2014

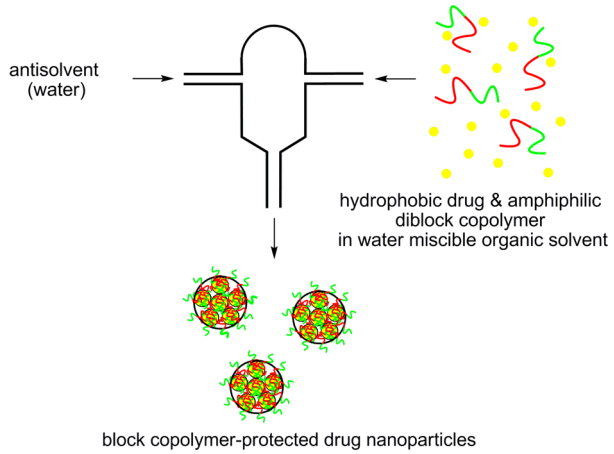

Figure 1. Schematic of impingement mixing to form block copolymer-protected nanoparticles (2D view of cross section).[26]

(ethylene glycol) (PLA-*b*-PEG), and poly(lactic-*co*-glycolic acid)-*block*-poly(ethylene glycol) (PLGA-*b*-PEG)],[22,27] have been explored to investigate their effects on the particle formation and stability. Up to now, little work[28] has been reported to investigate the effects of drug compounds on the particle stability, which will be discussed in this study. As demonstrated in our previous study,[27] biodegradable PLGA-*b*-PEG (Scheme 1) is a suitable steric stabilizer for the FNP to inhibit the particle aggregation, since the PLGA block is noncrystallizable as well as has relatively high glass transition temperature and a right solubility parameter (δ), ensuring that no unexpected particle destabilization introduced by this additive.[27] β-carotene, hydrocortisone, hydrocortisone ethoxysilicate, betulin, paclitaxel, and paclitaxel 2′,7-bis-(triethoxysilicate) will be used as the drugs. (Scheme 1) These compounds or their analogues are listed in the US National Cancer Institute (NCI) Drug Dictionary.[29] The aims of this study are to give a guideline to choose the suitable drug with good particle stability for flash nanoprecipitation especially at a high drug loading (e.g., > 40 wt %), to create an approach to predict the particle stability for a randomly selected drug structure, and to give a possible approach to improve the particle stability. For the purpose of predicting particle stability, the *n*-octanol/water partition coefficient (Log*P*), a hydrophobicity indication, will be introduced into the FNP technique. The properties of *n*-octanol has been thought to resemble to those of lipid bilayer membranes, suggesting to some extent that a drug partition in octanol/water simulates its ability to passively diffuse across biological membranes. Log*P* as a standard measurement of drug hydrophobicity has been widely used in the pharmaceutical industry. An empirical rule correlating Log*P* with the particle stability made via FNP will be given to help enable a fast preclinical drug prescreen.

EXPERIMENTAL SECTION

Materials. β-carotene is a type of antioxidant found in yellow and orange fruits and vegetables and in dark green, leafy vegetables. The body can make vitamin A from β-carotene. It is being studied in the prevention of some types of cancer.[29]

Hydrocortisone is a steroid hormone produced by the adrenal cortex with primary glucocorticoid and minor mineralocorticoid effects. As a glucocorticoid receptor agonist, hydrocortisone promotes protein catabolism, gluconeogenesis, capillary wall stability, and renal excretion of calcium and suppresses immune and inflammatory responses. Its synthetic counterpart is used, either as an injection or topically, in the treatment of inflammation, allergy, collagen diseases, asthma, adrenocortical deficiency, shock, and some neoplastic conditions.[29]

Betulin is isolated from the bark of betula alba, the common white birch. Its derivative, betulin acid, is a pentacyclic lupane-

Scheme 1. Structures of the Block Copolymer and Hydrophobic Drug Compounds

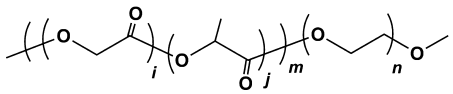

a) poly(lactic-*co*-glycolic acid)-*b*-poly(ethylene glycol) (PLGA-*b*-PEG)

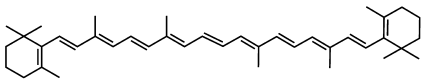

b) β-carotene

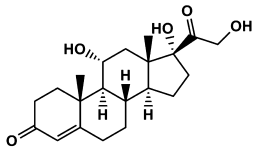

c1) Hydrocortisone

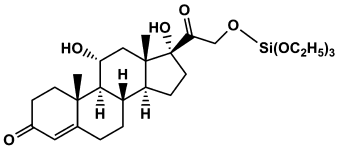

c2) Hydrocortisone Ethoxysilicate

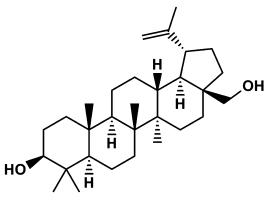

d) Betulin

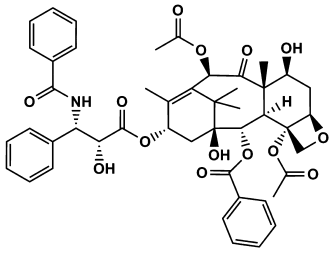

e1) Paclitaxel

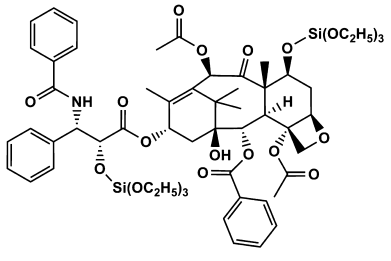

e2) Paclitaxel 2',7-Bis(triethoxysilicate)

dx.doi.org/10.1021/mp500025e | *Mol. Pharmaceutics* 2014, 11, 776−786

type triterpene with anti-inflammatory, anti-HIV, and anti-neoplastic activities. Betulinic acid induces apoptosis through induction of changes in mitochondrial membrane potential, production of reactive oxygen species, and opening of mitochondrial permeability transition pores, resulting in the release of mitochondrial apogenic factors, activation of caspases, and DNA fragmentation. Although originally thought to exhibit specific cytotoxicity against melanoma cells, this agent has been found to be also cytotoxic against nonmelanoma tumor cell types including neuroectodermal and brain tumor cells.[29]

Paclitaxel is a compound extracted from the pacific yew tree, *Taxus brevifolia*, with antineoplastic activity. It binds to tubulin and inhibits the disassembly of microtubules, thereby resulting in the inhibition of cell division. This agent also induces apoptosis by binding to and blocking the function of the apoptosis inhibitor protein B-cell Leukemia 2 (Bcl-2).[29]

β-carotene (≥97%), betulin (≥98%), water (HPLC grade), and tetrahydrofuran (THF, HPLC grade) were purchased from Aldrich and used as received. Paclitaxel was purchased from Polymed Therapeutics, Houston. Paclitaxel 2′,7-bis-(triethoxysilicate) and hydrocortisone ethoxysilicate were synthesized by Wohl[30] (see Scheme S1 in Supporting Information). Paclitaxel 2′,7-bis(triethoxysilicate) were chemically very stable in water in pH 7 but would hydrolyze in an acidic condition.[30]

PLGA(10k)-*b*-PEG(2k) was synthesized by the ring-opening polymerization of (D,L)-lactide and glycolide with mPEG(2k)-OH as the initiator and Tin(II) 2-ethylhexanoate as the catalyst in bulk at 150 °C. The obtained product was diluted in THF, dialyzed (Spectra/Pro 7 RC, molecular weight cut off (MWCO) of 1000) with CH_3OH for two days to remove unreacted monomers, and then concentrated under vacuum. $\bar{M}_n$ of PLGA(10k)-*b*-PEG(2k) was determined by NMR, and $\bar{M}_w/\bar{M}_n$ was determined by GPC as 1.46.[27] The PLGA blocks comprised 50% of lactic acid and 50% of glycolic acid confirmed by NMR and were amorphous.

Particle Preparation. The two-stream mixer and the FNP process are illustrated in Figure 1. The chamber dimensions were the same as those used by Johnson et al.[16] and Liu et al.[31] (type 500A-Y2X with dimensions described in Figure 4 and Table 1 in ref 16 and in Figure 1 in ref 31). In this study, the mixer was modified to allow unequal flow momentums from two opposite jets[24] (see Figure S1a in Supporting Information or Figure 3 in ref 24). Each mixer inlet was connected to a 10 mL of gastight glass syringe (SGE Inc.) via Teflon tubing with 1.6 mm ID. Both syringes were loaded on an infusion syringe pump (Harvard Apparatus model 975). For typical mixing, 25 mg of the drug compound and 25 mg of the BCP were dissolved in 5 mL of THF and were loaded in one syringe. Another syringe was loaded with 5 mL of H_2O. Two streams were impinged at a high velocity inside the mixer chamber. In most cases the flow rate was 72 mL/min which produces a mean jet velocity of 6.1 m/s through the 0.500 mm diameter nozzle. The outlet of the mixer was connected via 12.7 cm of 1.6 mm ID Teflon tubing to a beaker containing 90 mL of H_2O to further dilute the nanoparticles. The Reynolds number (Re),[32] a ratio of inertial force to viscous force, was used to quantify the mixing.

$$Re = \frac{\rho V a}{\eta} = \frac{\rho Q a}{s\eta} \tag{1}$$

where ρ is a fluid density, η is a fluid viscosity, V is a velocity, and Q is a flow rate. For jets mixing, a is a diameter of an inlet nozzle, and s is a cross sectional area of an inlet nozzle.[16,33,34] Re higher than a transition value, which mainly depends on a mixer design, indicates a sufficient mixing quality producing an asymptotic mean particle size.[18,27] Johnson and Prud'homme[17] reported that the transition of this T-mixer corresponded to a jet velocity of ∼2.1 m/s by mixing THF and water at 35 °C. With a room temperature correction to ρ and η, the jet velocity of 6.1 m/s in this study was still high enough for providing sufficient mixing. In most of the previous studies by others, the two stream jets mixer required an equal momentum from two opposite streams, and Re was usually reported with Re_1 of a single stream.[16,31] However, a four stream jets mixer allowed unequal momentums, and Re was usually reported by accumulating multiple streams.[20,23] In this study, the two stream jets mixer allowed unequal momentums from two opposite jets. The density (960 kg/m^3) and viscosity (1.66 mPa·s) of a 50:50 THF/water mixture[15] in the chamber were used to calculate Re, which to a certain extent was able to better compare with a situation of mixing two identical streams. A mean Re of 1770 for a single stream and the accumulation of 3540 for two therefore were calculated. The concentration of the final product in 95 mL of H_2O and 5 mL of THF was 0.05 wt %. The residence time was about 110 ms from entering the chamber to falling into the beaker. The total injection time was about 5 s.

All β-carotene experiments were done with a four-stream vortex mixer. The procedures were described in our previous work.[23,27] Typically two of the mixer inlets were connected to two gastight plastic syringes (60 mL, Kendall Monojet) via Teflon tubing with 1.6 mm ID. Each plastic syringe contained 45 mL of water and was driven by an infusion syringe pump (Harvard Apparatus, model 945). The other two inlets were connected to two gastight glass syringes (10 mL, SGE) via Teflon tubing. One of the syringes contained 5 mL of a β-carotene (50 mg) and BCP (50 mg) THF solution; another contained 5 mL of pure THF. The two glass syringes were driven by a second infusion syringe pump (Harvard Apparatus, PHD 2000 programmable). The pumps propel the four streams at high velocity into the small mixing chamber, generating high turbulence. Complete dimensions (see Figure S1b in Supporting Information or Figure 4 in ref 20) and evaluation of mixing performance using competitive reactions are given by Liu et al.[20] The flow rates were 120 mL/min for the plastic syringes and 13.3 mL/min for the glass syringes. From these flow rates, an Re of ∼3000 (higher than the transition value of ∼450[27]) was calculated, using the relation (eq 2) reported in refs 19 and 20:

$$Re = \sum_{i=1}^{4} Re_i = \sum_{i=1}^{4} \frac{\rho_i Q_i a_i}{s_i \eta_i} \tag{2}$$

where ρ_i is the density of the ith component, Q_i is the flow rate of the ith component, a_i in this study is the shorter width of the ith inlet nozzle (1.1×10^{-3} m), s_i is the cross sectional area of the ith inlet nozzle (1.65×10^{-6} m^2), and η_i is the viscosity of the ith component. The two water streams dominate Re, and this study assumes $\rho_i = 1.0 \times 10^3$ kg·m^{-3} and $\eta_i = 8.9 \times 10^{-4}$ Pa·s at room temperature. The outlet of the mixer was connected via a Teflon tubing to a beaker, where the nanosuspensions were collected without further dilution. The concentration of the final product in 90 mL of H_2O and 10 mL of THF was 0.1 wt %. The total injection time was about 23 s.

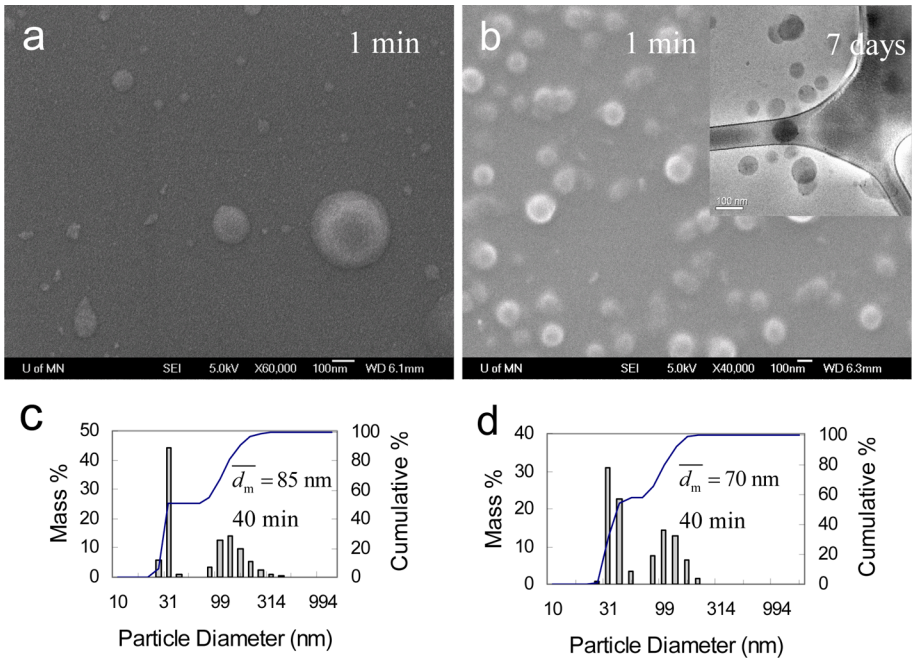

Figure 2. SEM images (cryo-TEM insert) and particle size distribution by DLS of PLGA(10k)-*b*-PEG(2k) (50 mg) nanoparticles (a, c) without, and (b, d) with β-carotene (50 mg) made with 10 mL of THF and 90 mL of H_2O (all scale bars are 100 nm).

Characterization. All samples were analyzed in the as-mixed liquid, water with 5−10% of THF, and also without and with 1 wt % of saline added to this THF/water solution. Saline was used to test the electrostatic stability of the particles; 1 wt % was chosen because it is similar to the ion concentration in body fluids. The particle size and distribution were determined by dynamic light scattering (DLS) using a ZetaPALS (Brookhaven Instruments, diode laser BI-DPSS wavelength of 659 nm, round cuvette). The light intensity correlation function was collected at 25 °C and a scattering angle of 90°. The correlation function is a combination of the diffusion coefficient, D_i, of each particle which is converted into particle diameter, d_i, with the Stokes−Einstein equation (eq 3),

$$d_i = \frac{k_b T}{3\pi\eta D_i} \tag{3}$$

where k_b is the Boltzmann constant and T is the absolute temperature. Correlation functions were downloaded from the ZetaPALS and fit using the REPES model. REPES yields a series of discrete particle diameters to represent the particle size distribution. It has been found more accurate than the cumulant model used in most commercial instruments. The software, GENDIST, was used to solve the REPES algorithm[35,36] and provided the size in an intensity distribution. The intensity averaged particle size, $\overline{d}_I$, is defined in eq 4,

$$\overline{d}_I = \sum n_i d_i^6 / \sum n_i d_i^5 \tag{4}$$

where n_i is the number of particles with a diameter of d_i. The mass averaged diameter, $\overline{d}_m$, is more practically useful than the usual intensity average for estimating drug loading and availability. It is defined in eq 5,

$$\overline{d}_m = \sum n_i m_i d_i / \sum n_i m_i = \sum n_i d_i^4 / \sum n_i d_i^3 \tag{5}$$

where m_i is the mass of a particle with a diameter of d_i. As discussed in our previous work,[23] the systematic errors including both reproducibility of mixing and property measurements were within ±10% for $\overline{d}_m$.

Cryogenic transmission electron microscopy (cryo-TEM) specimens were prepared as described also in ref 23 and were imaged at about −170 °C and 120 kV acceleration voltage by a Gatan US1000 cooled CCD camera. The scanning electron microscopy (SEM) specimens were prepared as described also in ref 23 and then were sputter-coated with a 30 Å layer of platinum and imaged with a JEOL 6500 SEM.

High-performance liquid chromatography (HPLC) was used to measure the concentration of the encapsulated paclitaxel in the nanoparticles and the free paclitaxel in THF and water mixture. The paclitaxel nanoparticles were removed from 0.5 mL of the suspension using a centrifugal filter (YM-100, Microcon) with a membrane cutoff of 100 kDa (8 nm pore size) under 12 000 × *g*. The filtrate was freeze-dried. Then 0.5 mL of THF was used to redisolve paclitaxel. The filtered nanoparticles were freeze-dried and extracted by 5 mL of methanol/THF (4:1) with stirring overnight. The carrier solvent was acetonitrile/ammonium acetate (10 mmol·L^{-1}) in water in pH 4 (adjusted with glacial acetic acid) (mobile phase ratio 55/45) eluted through a C18 RP (Beckman) HPLC column at a flow rate of 1 mL/min. The column pressure was 0.9 kpsi. The injection volume was 30 μL. The paclitaxel was detected by UV−Vis detector (Beckman 168) at the wavelength of 228 nm. The peak retention time was about 7 min, and the run time was 10 min. The C_{DL} % is defined as the ratio of the mass of the drug trapped in the nanoparticles to the total mass of the nanoparticles. C_{DL} % of paclitaxel was 55 wt % by HPLC. 90.2% of paclitaxel was precipitated as the nanoparticles, and 9.8% was in free molecules in the filtrate.

δ were calculated with the Hoye method.[37] The chemical structures were drawn by ACD/ChemSketch (Freeware downloaded from www.acdlabs.com, product version 12.01), and their Log*P* were calculated with the ACDLog*P* add-on.

dx.doi.org/10.1021/mp500025e | *Mol. Pharmaceutics* 2014, 11, 776−786

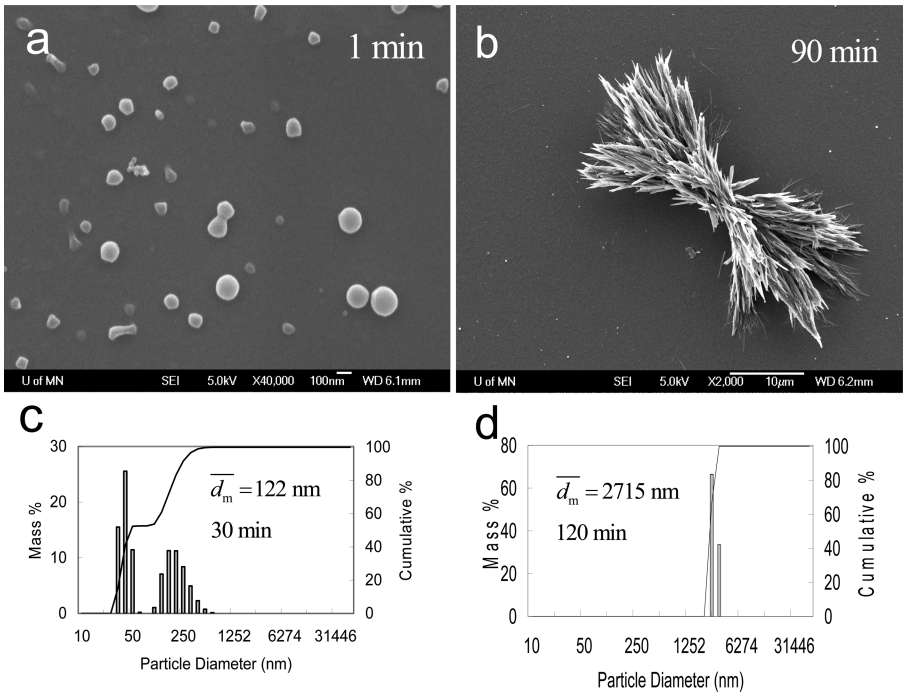

Figure 3. SEM images of PLGA(10k)-*b*-PEG(2k) (25 mg)/paclitaxel (25 mg) nanoparticles made with 5 mL of THF and 95 mL of H_2O (a) sprayed within 1 min on a silicon wafer (the scale bar is 100 nm) and (b) sprayed within 90 min, showing grown paclitaxel needles (the scale bar is 10 μm). Particle size and distribution (c) in 30 min and (d) in 120 min.

RESULTS AND DISCUSSION

Nanoparticle Stability. There are three sources of nanoparticle instability, i.e., aggregation, Ostwald ripening, and recrystallization. As discussed in our previous work, polyelectrolytes, such as chitosan,[23] or amphiphilic BCPs, such as PLGA-*b*-PEG,[27] were able to effectively hinder the nanoparticle aggregation. In this study, PLGA-*b*-PEG was used as a model surfactant, whose hydrophobic block was non-crystallizable as well as had relatively high glass transition temperature and a right solubility parameter, ensuring no unexpected particle destabilization is introduced by this additive.[27] It was also showed that the molecular weights of the PLGA block over the range from 5k to 15k and the PEG block over the range from 2k to 5k had insignificant effects on the particle stability.[27] PLGA(10k)-*b*-PEG(2k) was used in this study, and Figure 2 showed PLGA(10k)-*b*-PEG(2k) nanoparticles made via FNP either without or with β-carotene. The PLGA-*b*-PEG/β-carotene particles were relatively stable for at least 3 weeks with the size slowly increasing from 57 to 90 nm.[27]

Ostwald ripening is the phenomenon by which small particles are essentially consumed by large particles during the growth process, since the small particles have a higher solubility than the large particles as described by the Kelvin equation.[38] The driving force is to lower the surface energy. It usually facilitates the interparticle recrystallization. Ostwald ripening was first described by Lifshitz, Slyozov, and Wagner (LSW).[39,40] For a diffusion-controlled process, the average radius of the particles, $\overline{r}$, changes with time according to

$$\overline{r} = \sqrt[3]{Kt} = \sqrt[3]{\frac{8\sigma D\nu C_{eq} t}{9k_b T \ln S}} = \sqrt[3]{\frac{8\sigma D\nu C_{eq} t}{9k_b T \ln(C/C_{eq})}} \quad (6)$$

$$\frac{d\overline{r}}{dt} = \frac{1}{3}\sqrt[3]{\frac{8\sigma D\nu C_{eq}}{9k_b T t^2 \ln(C/C_{eq})}} \quad (7)$$

where K is a rate constant, σ is an interfacial energy, D is a diffusion coefficient of the solute molecule, ν is a volume of a solute molecule, t is time, C_{eq} is a solute solubility, C is a solute concentration, and S is a supersaturation ratio, C/C_{eq}. All values are in terms of the solution, such as the mixture of 10 vol % of THF and 90 vol % of H_2O (noted as 1THF/9H_2O) used in this study. The particle size is thus proportional to $t^{1/3}$. With a specific drug compound, only C_{eq} and C alter the coarsening rate, $d\overline{r}/dt$. With a constant C, increasing the ratio of the organic solvent over water increases C_{eq} and thus $d\overline{r}/dt$. To inhibit the Ostwald ripening for a given hydrophobic drug, therefore, a minimum usage of the organic solvent is desired. For most hydrophobic drugs, the range of σ, D, and ν typically are less than 10-fold. However, the difference of C_{eq} can vary much larger than 10-fold. C_{eq} dominates the Ostwald ripening, and a lower C_{eq} is desired for the stability.

In experiments, the solubility of paclitaxel was 25 $\mu g \cdot mL^{-1}$ in 1THF/19H_2O.[23] The PLGA-*b*-PEG/paclitaxel nanoparticles grew from about 100 nm to tens of micrometers within 90 min (see Figure 3a and b). β-carotene had a solubility of 3.1 ng·mL^{-1} in 1THF/9H_2O. The β-carotene particles without adding any stabilizer spent about four hours growing from 89 nm to about 180 nm, and all of the particles sedimented on the bottom with the colorless supernatant within one day.[23] With PLGA-*b*-PEG, the particle size slowly increased from 57 to 90 nm in 3 weeks[27] and was much more stable than PLGA-*b*-PEG/paclitaxel nanoparticles. Paclitaxel 2′,7-bis-(triethoxysilicate) even had a lower solubility, was out of the detection limit of HPLC, and was not able to be obtained in this study (<1 ng·mL^{-1}). The particles spent 8 days growing from 55 to 153 nm (see Figure 4c and d). With PLGA-*b*-PEG,

dx.doi.org/10.1021/mp500025e | *Mol. Pharmaceutics* 2014, 11, 776−786

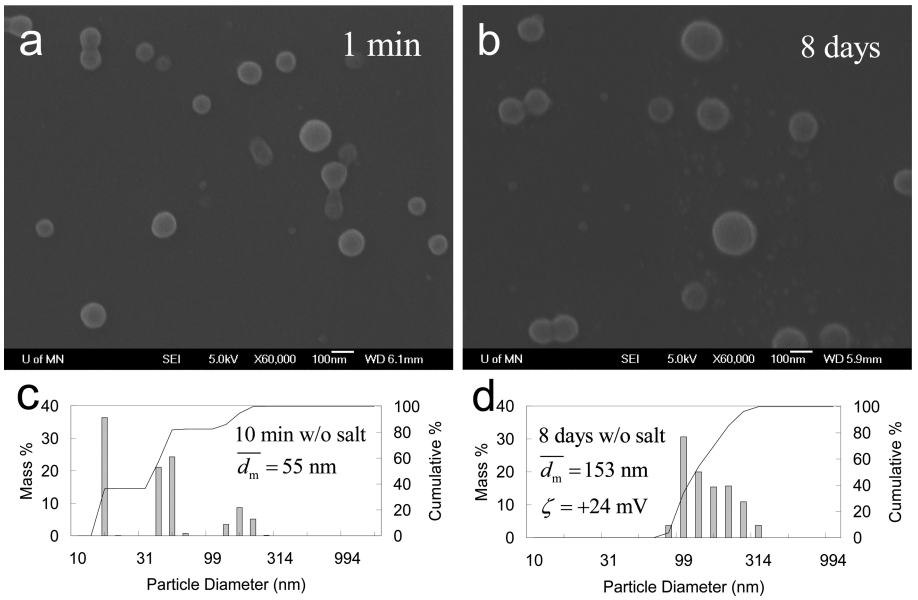

Figure 4. SEM images of paclitaxel 2′,7-bis(triethoxysilicate) (35 mg, molar equivalent to 25 mg of paclitaxel) nanoparticles made with 5 mL of THF and 95 mL of H_2O (a) sprayed within 1 min on a silicon wafer and (b) sprayed in 8 days (both scale bars are 100 nm). Particle size and distribution w/o saline (c) in 10 min and (d) in 8 days. ζ = +24 mV before adding saline, and the nanoparticles grew to visually detectable size instantly after adding 1 wt % saline and had ζ = +2.8 mV.

the particle size slowly increased from 86 to 102 nm in 6 days (see Figure 5b). These comparisons showed that by changing the drug solute, the lower the drug solubility in the aqueous medium, the more stable the particles made via FNP. This observation was consistent with the prediction by the LSW theory above that C_{eq} dominated the Ostwald ripening, and a lower C_{eq} was desired for the stability. Also it was consistent with the study by Liu et al. on Ostwald ripening of β-carotene nanoparticles where the β-carotene nanoparticles were made via FNP but changing the ratio of THF over water. They made the same conclusion that with FNP the lower the solute solubility in the mixture, the slower the growth rate of the particles.

As described by the Kelvin equation (eq 8), small particles have a higher solubility than large particles.

$$C_{eq}(r) = C_{eq}(\infty)\exp\left(\frac{2\sigma v}{rk_bT}\right) = C_{eq}(\infty)\exp\left(\frac{l}{r}\right) \quad (8)$$

where $C_{eq}(r)$ is a solubility surrounding a particle of a radius r, and $C_{eq}(\infty)$ is a bulk solubility. The capillary length, l, is a characteristic length below which curvature-induced solubility is significant and defined as $l \equiv 2\sigma v/k_bT$. As predicted by the LSW theory, a higher C_{eq} of small particles is able to accelerate Ostwald ripening. Therefore, the initial particle size distribution is expected to have an effect in some degree on the particle stability and is discussed here.

With BCPs, the particles of a hydrophobic drug made via FNP were believed to be surrounded by amphiphilic BCPs via a kinetic process during drug precipitation,[18,21,27] and the interfacial energy of the particles was reported by Johnson et al. as $\sigma = 1.9 \times 10^{-3}$ J·m^{-2}.[18] Liu et al. used this value and well predicted Ostwald ripening of PEGylated BCP protected β-carotene nanoparticles in THF/water (6/120−30/120) mixtures.[21] This value is thus taken herein. With a molecular weight of 854 g·mol^{-1} and an assumption of the drug density of 1.0×10^3 kg·m^{-3}, ν of 1.42×10^{-27} m^3·molecule^{-1} and l of 1.33 nm at room temperature can be estimated. Since $l/r \ll 1$, eq 8 can be linearized into eq 9.

$$C_{eq}(r) \approx C_{eq}(\infty)\left(1 + \frac{l}{r}\right) \quad (9)$$

If the particle size distribution at 30 min given by DLS in Figure 3c is considered as the initial distribution of the PLGA-*b*-PEG/paclitaxel nanoparticles, the solubility ratio of the lower radius limit (r_{min}) over the upper (r_{max}), C_{eq}(16 nm)/C_{eq}(314 nm), was calculated as 1.08. Without BCPs, paclitaxel nanoparticles had $\sigma = \gamma_{water} - \gamma_{drug} = 7.28 \times 10^{-2} - 6.85 \times 10^{-2} = 4.3 \times 10^{-3}$ J·m^{-2} (surface tension of drug $\gamma_{drug} = 6.85 \times 10^{-2}$ J·m^{-2} calculated with ACD/I-Lab). l of 3.02 nm and C_{eq}(16 nm)/C_{eq}(314 nm) of 1.18 were also calculated. Compared with solubility changes by using other drugs, this small solubility difference ($C_{eq}(r_{min})/C_{eq}(r_{max}) \approx 1$) between large and small paclitaxel particles was insignificant. Therefore, for PLGA-*b*-PEG/paclitaxel nanoparticles the effect of the particle size distribution on Ostwald ripening was negligible.

For β-carotene itself, nanoparticles[27] had $\sigma = \gamma_{water} - \gamma_{drug} = 3.65 \times 10^{-2}$ J·m^{-2} ($\gamma_{drug} = 3.63 \times 10^{-2}$ J·m^{-2} calculated with ACD/I-Lab) and molecular weight of 537 g·mol^{-1}. l of 16.1 nm and C_{eq}(13 nm)/C_{eq}(249 nm) of 3.23 at 10 min were estimated by eq 8. In the same way, for paclitaxel 2′,7-bis(triethoxysilicate) nanoparticles (see Figure 4c) with $\sigma = \gamma_{water} - \gamma_{drug} = 2.05 \times 10^{-2}$ J·m^{-2} ($\gamma_{drug} = 5.23 \times 10^{-2}$ J·m^{-2} calculated with ACD/I-Lab) and molecular weight of 1178 g·mol^{-1}, l of 19.8 nm and C_{eq}(8 nm)/C_{eq}(125 nm) of 10.1 at 10 min were estimated. By comparing the initial $C_{eq}(r_{min})/C_{eq}(r_{max})$, PLGA-*b*-PEG/paclitaxel nanoparticles (1.08) < β-carotene nanoparticles (3.23) < paclitaxel 2′,7-bis(triethoxysilicate) nanoparticles (10.1). As predicted by the LSW theory, the stability trend should be PLGA-*b*-PEG/paclitaxel nanoparticles > β-carotene nanoparticles > paclitaxel 2′,7-bis(triethoxysilicate) nanoparticles. However, this stability trend was opposite to the observed trend. Therefore, compared with the solubility changes by using different drugs, the

dx.doi.org/10.1021/mp500025e | *Mol. Pharmaceutics* 2014, 11, 776−786

solubility difference between the small and the large particles made via FNP was considered to have an insignificant effect on the particle stability. The particle size distributions were narrow enough in terms of Ostwald ripening to study particle stability.

The third instability source is recrystallization, which converts amorphous particles into crystalline ones, since amorphous drugs have a higher solubility than the crystalline counterparts. The driving force is to lower the free energy of the solid state. It is a reorganization process of the precipitated solute molecules. Solvent molecules dissolved in the solute matrix provide free volume, facilitate the relaxation of the solute, and increase the rate of recrystallization inside the particles. Since intraparticle recrystallization barely changes the nanoparticle volume and all instable systems in this study showed a significant volume increase of individual particles, intraparticle recrystallization would not be studied in this paper. However, interparticle recrystallization is able to significantly increase the particle volume. The process requires solute molecules migrate from one particle to another via either Ostwald ripening or particle aggregation. By adding surface steric stabilizer, such as PLGA-*b*-PEG, particle aggregation can be effectively hindered. Ostwald ripening again as the source of particle instability and shown above has to be considered in this study.

Enhanced Stability with Chemical Modification. As discussed above with the LSW theory, the solubility of C_{eq} plays an important role on nanoparticle stability. For a given drug compound, the water solubility can be decreased by (1) decreasing the ratio of organic solvent over water,[19,21] (2) choosing a relatively poor organic solvent, or (3) being chemically modified, such as bonding to a hydrophobic moiety or form a salt. However, the amount of organic solvent was limited by the solubility of a drug in it and processing conditions during feeding and cannot be infinitely decreased. Feeding more water to decrease the ratio of organic solvent over water will dilute the product too much, and the concentration is too low. The option of organic solvents is limited by water miscibility, solvent toxicity, and easiness of solvent removal. Moreover, some drugs are relatively too water-soluble. A possible approach is to modify the chemical structure of the drug and make it less soluble. In this study, therefore, paclitaxel was chemically bonded with ethoxysilicate (see Scheme S1a in Supporting Information), which was a hydrophobic moiety and was expected to be easily cleaved under an acidic condition in tumors. Much work on hydrolysis of various paclitaxel organosilicate vs pH was studied by Wohl[30] and showed promising results for a controlled release in a mimic condition of tumor cells. While at neutral pH, it was chemically very stable. In this study, as shown in Figure 4c and d, even without the steric stabilizer of PLGA-*b*-PEG, $\overline{d}_m$ of the paclitaxel 2′,7-bis(triethoxysilicate) nanoparticles only increased from 55 to 153 nm in 8 days, showing significant improvement of the particle stability compared with PLGA-*b*-PEG/paclitaxel particles with grown micrometer needles in 90 min (see Figure 3b). Figure 4a and b showed that the particles remain spherical for at least 8 days. The improved stability in the morphology and the size indicated that the Ostwald ripening and recrystallization were significantly inhibited. The strategy of chemical bonding the marginally hydrophobic drug with hydrophobic moieties succeeded.

It was found that the paclitaxel 2′,7-bis(triethoxysilicate) nanoparticles without the stabilizer had surface charges (ζ = +24 mV) to inhibit the aggregation. After adding 1 wt % saline, however, ζ decreased to +2.8 mV. The nanoparticles grew rapidly and became visually detectable. The steric stabilizer, PLGA-*b*-PEG, was thus used to inhibit the aggregation. As shown in Figure 5b, the particles had a good stability with size

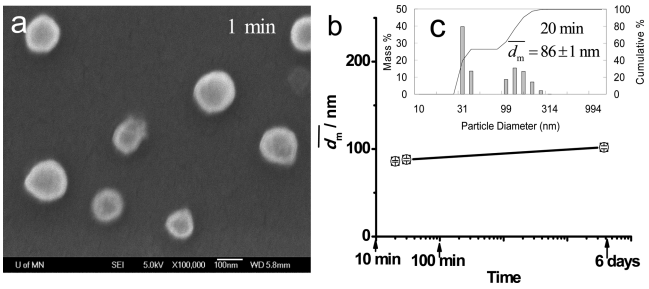

Figure 5. PLGA(10k)-*b*-PEG(2k) (25 mg) protected paclitaxel 2′,7-bis(triethoxysilicate) (35 mg, molar equivalent to 25 mg of paclitaxel) nanoparticles made with 5 mL of THF and 95 mL of H_2O and (a) sprayed within 1 min on a silicon wafer (the scale bar is 100 nm); (b) particle stability against time for 6 days; (c) particle size distribution by DLS in 20 min without saline. No noticeable size increase after adding saline in the 6th day, indicating the nanoparticles were sterically stabilized by PLGA(10k)-*b*-PEG(2k).

increasing from 86 to 102 nm after 6 days without saline. After adding 1 wt % saline in the 6th day, no visible aggregation was observed. The DLS showed that the size barely changed.

Stability Prediction. As described with the LSW theory as well as observed in above experiments, the solubility of a hydrophobic compound has dominant effects on the stability of the formed nanoparticles in terms of Ostwald ripening and interparticle recrystallization. For a random given drug to generate nanoparticles via the FNP, it would be good to measure first the solubility in the solvent/antisolvent mixture. If changing the ratio of the solvent to antisolvent is necessary to optimize the process, a phase diagram is desired as well. In practice, however, measuring the solubility and stability could be very time-consuming, a quantitative relation between solubility with stability is unclear, and generated nanoparticles are not necessarily sufficiently stable. Therefore, having a theoretical indication of the solubility, the correlation of this indication with the particle stability and then a prediction of the stability are very meaningful. This approach is also very useful to give a guideline before doing any chemical modification of a drug compound.

In this study, two well-known physical parameters, Hildebrand solubility parameter (δ)[41] and Log*P*,[42] were investigated to tentatively build the correlation between the solubility and the stability. δ provides a numerical estimate of the degree of interaction between materials, particularly for nonpolar materials such as many polymers. Materials with similar values of δ are likely to be miscible. It can be a good indication of solubility. As well, the lower δ is, the higher the hydrophobicity is. The octanol−water partition coefficient is a ratio of concentrations of un-ionized compound between immiscible octanol with water. The logarithm of the partition coefficient is called Log*P*. It is one of simple molecular descriptors in Lipinski's "Rule of 5".[1] It serves as a quantitative indication of lipophilicity and has been widely employed in the pharmaceutical industry.

Hydrocortisone, hydrocortisone ethoxysilicate, and betulin were therefore added to the list for the correlation study. As reported, hydrocortisone has a water solubility of 0.3 mg/

mL.[43,44] After adding 10 vol % of good solvent, i.e.,THF, the solubility would be much higher. As expected, 50 mg of hydrocortison in 10 mL of THF and 90 mL of H_2O did not generate a detectable scattered intensity by DLS, indicating nanoparticles were not generated since the solubility was too high. Its analogue, hydrocortisone ethoxysilicate, was thus synthesized to increase the hydrophobicity and lower the solubility. The nanoparticles (50 mg) of hydrocortisone ethoxysilicate had $\bar{d}_m$ of 252 nm after 10 min than the formation in 10 mL of THF and 90 mL of H_2O and showed fast increasing size in the next 10 min during the DLS measurement. Unfortunately, hydrocortisone ethoxysilicate hydrolyzed fast back into more hydrophilic hydrocortisone, and the nanoparticle size decreased as the time went during the next six days (see Figure S2 in Supporting Information). It therefore was not a good candidate for studying the nanoparticle stability herein but able to give another example of the fast size increase at least in the first 20 min.

For betulin, like paclitaxel in Figure 3, the nanoparticles were not stable. The suspension changed from water clear to cloudy with visible needles within 30 min, indicating fast Ostwald ripening and recrystallization. The SEM image (see Figure S3 in Supporting Information) showed grown crystalline needles sprayed on a silicon wafer within 30 min after mixing.

Table 1 listed δ and Log*P* of the drugs or their analogues. δ did not show a good correlation with the nanoparticle stability.

Table 1. ACDLog*P* and δ of Various Organic Compounds against Nanoparticle Stability

organic compound	δ^a ($MPa^{1/2}$)	ACDLog*P*	stable (Y/N)
hydrocortisone	23.2	1.43 ± 0.47	no particle
odanacatib	29.7	2.92 ± 0.85	N[28]
curcumin	22.8	2.92 ± 0.48	N
itraconazol	19.1	4.35 ± 1.22	N[28]
hydrocortisone ethoxysilicate	21.2	6.37 ± 0.72	N
paclitaxel	22.3	7.38 ± 0.83	N
betulin	18.7	9.01 ± 0.39	N
vitamin E succinate	18.5	11.88 ± 0.30	Y[45]
paclitaxel 2′-triethoxysilicate	21.4	13.09 ± 1.00	Y[30]
paclitaxel 2′-tri*i*-propoxysilicate	21.0	14.13 ± 1.01	Y[30]
β-carotene	17.8	15.51 ± 0.43	Y
paclitaxel 2′,7-bis(triethoxysilicate)	20.8	18.36 ± 1.15	Y
tetramenthoxysilane	16.7	18.66 ± 0.66	Y[30]

[a]Estimated with the Hoye method as well as assumed to treat the Si atom as a C atom.

The reason could come from the limitation of δ, which was not suitable for polar compounds especially with hydrogen bonds (such as water).[41,46,47] On the contrary, Log*P* showed a good correlation. Empirically, with ACDLog*P* > ∼12, nanoparticles showed good stability; with ∼2 < ACDLog*P* < ∼9, nanoparticles showed fast Ostwald ripening and recrystallization; with ACDLog*P* < ∼2, the drug is too soluble and very likely difficult to generate nanoparticles. In order to fill the gap of this rule, over 2000 anticancer drugs in the NCI dictionary were also screened, and very few real drugs have been found to have ACDLog*P* of greater than 9, since most of the super hydrophobic potential drugs had been abandoned by the pharmaceutical industry due to an extremely low dissolution rate. But one would reasonably expect that a drug with ∼9 < ACDLog*P* < ∼12 is marginal.

Rule Limitations. It was found that without adding any surface stabilizer β-carotene particles made via FNP showed good short-term (∼4 h) stability due to slightly negative surface charge[48] as judged by zeta potential measurements.[23] Paclitaxel 2′,7-bis(triethoxysilicate) particles in this study (see Figure 4) showed no sediment for 8 days. Compared with the time of the measurements and possible postprocessing, this stability was long enough. By using β-carotene therein, the effects of the hydrophobic drug on particle instability were able to be removed so as the effects of mixer designs,[24] mixing processes,[23,27] and surface stabilizers[23,27] can be individually studied. It was also found that even with sufficient mixing some polymeric stabilizers (e.g., PLA-*b*-PEG and PCL-*b*-PEG) destabilized the particles due to their undesired physical properties (e.g., relatively low glass transition, polymer crystallization, and unsuitable solubility parameters).[27] However, PLGA-*b*-PEG, an amphiphilic diblock copolymer, had no negative impact on β-carotene particle stability. Moreover, with very similar experimental conditions of this study, the molecular weight of PLGA block over the range from 5k to 15k showed an insignificant effect on controlling the particle stability.[27] PLGA-*b*-PEG as a model polymeric surfactant therefore was used in this study to investigate the effects of the hydrophobic drugs. The empirical rule above was based on this surfactant, which did not have undesired physical properties to rather destabilize the particles like PCL-*b*-PEG or PLA-*b*-PEG.[27]

It is known that the solubility of a drug in the water/solvent mixture also depends on the type of a solvent and a feed ratio with water. The drug and polymer have to be molecularly dissolved in a solvent before jets mixing with water. With a fixed amount of drug or polymer, the solvent had a minimum amount. However, adding too much solvent required much more water to obtain either a high drug recovery or a stable nanosuspension with limited Ostwald ripening and recrystallization, which decreased the final concentration of the drug suspension. It has been found that in the FNP technique for β-carotene, paclitaxel and its prodrugs, 50 mg of a drug (or with extra 10 to 50 mg of a polymer) dissolving in 10 mL of a solvent and mixed with 90 mL of water (0.5 mg/mL of a drug in production) was the most suitable combination.[19,21−23,27,30] The above empirical rule was based on this combination at room temperature. For some cases, water was doubled in purpose, but no further dilution was taken, which would trouble the particle postprocessing by freeze or spray drying. In Table 2, ACDLog*P* and boiling point of common water miscible organic solvents were listed. THF was a relative hydrophobic solvent, and a good solvent for many organic drugs as well as for many common polymers. For drugs with ACDLog*P* > ∼2, acetone was tested with paclitaxel and its multiple prodrugs.[30] Their stability still well followed this empirical rule. For drugs with ACDLog*P* < ∼2, a less hydrophobic solvent such as acetone, ethanol (with ACDLog*P* slightly lower than zero), or their mixture with THF can be considered to generate instable naoparticles, which could decrease this empirical value. But a value of no less than zero is still expected.

It should be noted that Log*P* of a substance is most relevant for neutral substances and is useful as a general reference point to help compare overall hydrophobicity trends of compounds. Log*P* does not account for modifications in the hydrophobicity of ionizable compounds at varying pH. The appropriate descriptor for these compounds is the distribution coefficient, *D* (also typically used in its logarithmic form, log*D*).[49] Since the

dx.doi.org/10.1021/mp500025e | *Mol. Pharmaceutics* 2014, 11, 776−786

Table 2. ACDLog*P* and Boiling Point of Water, Octanol, and Various Water Miscible Organic Solvents

water miscible solvent/antisolvent	boiling point[a] (°C)	ACDLog*P*
methanol	65	−0.72 ± 0.18
ethanol	78	−0.19 ± 0.18
n-propanol	97	0.34 ± 0.18
ethylene glycol	197	−1.69 ± 0.21
1,2-propylene glycol	187	−1.34 ± 0.22
glycerin	182	−2.32 ± 0.49
acetonitrile	81	−0.45 ± 0.19
acetone	56	−0.16 ± 0.19
dimethyl sulfoxide (DMSO)	189	−1.35 ± 0.28
N,*N*-dimethylformamide (DMF)	153	−1.01 ± 0.28
tetrahydrofuran (THF)	66	0.33 ± 0.22
hexafluoroisopropanol (HFIP)	59	1.91 ± 0.79
water	100	−1.38 ± 0.21
n-octanol (water immiscible)	196	3.00 ± 0.18

[a]From Sigma Aldrich Inc.

software to calculate log*D* is not free for the public, Log*P* would be better to demonstrate this work to the interested readers. The algorithm model used in this study is ACDLog*P* developed by the ACD company, since this model has been used by some of the world's largest pharmaceutical companies (e.g., GlaxoSmithKline and Pfizer) and the ACD company also developed Log*D* model. There are various similar algorithm models available (e.g., ALog*P*, ALog*P*s, ABLog*P*, AClog*P*, COSMOFraq, cLog*P*, MlogP, MiLog*P*, ProLogP, XLog*P*, and Log*KOW*). Each algorithm model has its own strengths and exceptions,[50,51] but the comparable Log*D* model is not developed for all Log*P* models. Depending on the water miscible organic solvent used in the FNP (e.g., THF, acetone, ethanol, or their mixtures), different algorithm models of Log*P* possibly need to be tested for the exceptions.

CONCLUSION

In this study, the effects of the hydrophobic drug molecules on particle stability were investigated. The work demonstrated that chemically bonding a drug compound (e.g., paclitaxel) with a cleavable hydrophobic moiety of organosilicate (e.g., triethoxysilicate) was able to significantly improve the particle stability, expectedly due to a decreased drug solubility and thus lowered interparticle molecular migration. This modification opened an approach to enhance the particle stability generated by FNP. Even without any surfactant but with slight surface charges, paclitaxel 2′,7-bis(triethoxysilicate) nanoparticles showed moderate stability (no sediment for 8 days). To better stabilize the particles, PLGA-*b*-PEG was used as a model surface stabilizer, whose hydrophobic block was noncrystallizable as well as had relatively high glass transition temperature and a right solubility parameter, ensuring no unexpected particle destabilization introduced by this additive.[27]

By changing the solute with various drugs mostly from the NCI drug dictionary and their analogues, the study showed that the lower the solubility in the aqueous medium the greater the particle stability in terms of Ostwald ripening, which was consistent with the prediction by the LSW theory. The particle size distribution made via FNP was sufficient narrow. Compared with a solubility change by using a different drug solute, the particle solubility between small and large particles showed a negligible effect on Ostwald ripening.

The experiments showed that the initial particle size distribution made via FNP was bimodal or even trimodal rather than lognormal. Since the DLS apparatus typically cannot differentiate size peaks within 3-fold, in some case the distribution appeared unimodal. Very little has been known about the FNP kinetics which evolves in micro to miliseconds and a nanoscale. This study considers the non-lognormal and non-unimodal size distribution as evidence for "cluster−cluster aggregation"[22,27] rather than "nucleation and growth".[18]

To correlate the drug hydrophobicity with particle stability, δ and Log*P* were used as hydrophobicity indications for the drug compounds. Log*P* showed a good correlation with the nanoparticle stability. Empirically, with ACDLog*P* > ∼12, nanoparticles showed good stability; with ∼2 < ACDLog*P* < ∼9, nanoparticles showed fast Ostwald ripening and interparticle recrystallization; with ACDLog*P* < ∼2, the drug was too soluble and very likely difficult to generate nanoparticles. With ∼9 < ACDLog*P* < ∼12, the drug was expected to be marginal. This work introduced Log*P* into the flash nanoprecipitation, created a quick way to predict particle stability for a randomly selected drug structure enabling a fast preclinical drug screen, and provided a possible approach to enhance the particle stability. The limitations of the rule were also discussed.

ASSOCIATED CONTENT

Supporting Information

The information includes (1) scheme of synthesizing paclitaxel 2′,7-bis(triethoxysilicate) and hydrocortisone ethoxysilicate; (2) dimensions of the mixers; (3) stability of hydrocortisone silicate nanoparticles; (4) SEM images of betulin. This material is available free of charge via the Internet at http://pubs.acs.org.

AUTHOR INFORMATION

Corresponding Author

*Phone: 01-(612) 626-1005. E-mail: zhuxx086@umn.edu.

Notes

The authors declare no competing financial interest.

ACKNOWLEDGMENTS

The work partially references Chapter 5 of author's dissertation[26] in June 2010 at the University of Minnesota. The author thanks Dr. Chris Macosko for reviewing the manuscript, Adam Wohl for helping synthesize part of the materials, Jayanth Panyam and Haitao Qian for fruitful discussions, Udaya Toti for assisting in the HPLC measurement, Yeshayahu Talmon for taking the cryo-TEM image, and Michael Tsapatsis for the access of DLS apparatus. The work was supported by the US National Science Foundation under the NIRT Program (award number CTS-0506966), IPRIME and NSF-MRSEC at the University of Minnesota, the Lady Davis Fellowship Foundation at the Technion of Israel, the Minnesota Futures Grant Program, and the US National Institutes of Health (award number R21-EB011671). Parts of this work were carried out in the University of Minnesota College of Science and Engineering Characterization Facility, which receives partial support from NSF through the NNIN program.

REFERENCES

(1) Lipinski, C. A. Poor aqueous solubility - an industry wide problem in drug discovery. *Am. Pharm. Rev.* **2002**, *5*, 82−85.

(2) Muller, R. H.; Jacobs, C.; Kayser, O. Nanosuspensions as particulate drug formulations in therapy Rationale for development and what we can expect for the future. *Adv. Drug Delivery Rev.* **2001**, *47*, 3−19.
(3) Haag, R.; Kratz, F. Polymer therapeutics: Concepts and applications. *Angew. Chem., Int. Ed.* **2006**, *45*, 1198−1215.
(4) Discher, D. E.; Eisenberg, A. Polymer vesicles. *Science* **2002**, *297*, 967−973.
(5) Savic, R.; Luo, L. B.; Eisenberg, A.; Maysinger, D. Micellar nanocontainers distribute to defined cytoplasmic organelles. *Science* **2003**, *300*, 615−618.
(6) Jun, Y. J.; Toti, U. S.; Kim, H. Y.; Yu, J. Y.; Jeong, B.; Jun, M. J.; Sohn, Y. S. Thermoresponsive micelles from oligopeptide-grafted cyclotriphosphazenes. *Angew. Chem., Int. Ed.* **2006**, *45*, 6173−6176.
(7) Toti, U. S.; Moon, S. H.; Kim, H. Y.; Jun, Y. J.; Kim, B. M.; Park, Y. M.; Jeong, B.; Sohn, Y. S. Thermosensitive and biocompatible cyclotriphosphazene micelles. *J. Controlled Release* **2007**, *119*, 34−40.
(8) Lian, T.; Ho, R. J. Trends and developments in liposome drug delivery systems. *J. Pharm. Sci.* **2001**, *90*, 667−680.
(9) Ghoroghchian, P. P.; Frail, P. R.; Susumu, K.; Blessington, D.; Brannan, A. K.; Bates, F. S.; Chance, B.; Hammer, D. A.; Therien, M. J. Near-infrared-emissive polymersomes: self-assembled soft matter for in vivo optical imaging. *Proc. Natl. Acad. Sci. U.S.A.* **2005**, *102*, 2922−2927.
(10) Tamilvanan, S. Oil-in-water lipid emulsions: implications for parenteral and ocular delivering systems. *Prog. Lipid Res.* **2004**, *43*, 489−533.
(11) Horn, D.; Rieger, J. Organic nanoparticles in the aqueous phase - theory, experiment, and use. *Angew. Chem., Int. Ed.* **2001**, *40*, 4331−4361.
(12) Rabinow, B. E. Nanosuspensions in drug delivery. *Nat. Rev. Drug Discovery* **2004**, *3*, 785−796.
(13) Patil, Y.; Panyam, J. Polymeric nanoparticles for siRNA delivery and gene silencing. *Int. J. Pharmaceutics* **2009**, *367*, 195−203.
(14) Patil, Y. B.; Toti, U. S.; Khdair, A.; Ma, L.; Panyam, J. Single-step surface functionalization of polymeric nanoparticles for targeted drug delivery. *Biomaterials* **2009**, *30*, 859−866.
(15) Johnson, B. K. Flash nanoprecipitation of organic actives via confined micromixing and block copolymer stabilization. Ph.D. Dissertation, Princeton University, Princeton, 2003.
(16) Johnson, B. K.; Prud'homme, R. K. Chemical processing and micromixing in confined impinging jets. *AIChE J.* **2003**, *49*, 2264−2282.
(17) Johnson, B. K.; Prud'homme, R. K. Flash NanoPrecipitation of organic actives and block copolymers using a confined impinging jets mixer. *Aust. J. Chem.* **2003**, 1021−1024.
(18) Johnson, B. K.; Prud'homme, R. K. Mechanism for rapid self-assembly of block copolymer nanoparticles. *Phys. Rev. Lett.* **2003**, *91*, 1183021−1183024.
(19) Liu, Y. Formulation nanoparticles by flash nanoprecipitation for drug delivery and sustained release. Ph.D. Dissertation, Princeton University, Princeton, 2007.
(20) Liu, Y.; Cheng, C. Y.; Prud'homme, R. K.; Fox, R. O. Mixing in a multi-inlet vortex mixer (MIVM) for flash nano-precipitation. *Chem. Eng. Sci.* **2008**, *63*, 2829−2842.
(21) Liu, Y.; Kathan, K.; Saad, W.; Prud'homme, R. K. Ostwald ripening of beta-carotene nanoparticles. *Phys. Rev. Lett.* **2007**, *98*, 0361021−0361024.
(22) Zhu, Z. X.; Anacker, J. L.; Ji, S. X.; Hoye, T. R.; Macosko, C. W.; Prud'homme, R. K. Formation of block copolymer-protected nanoparticles via reactive impingement mixing. *Langmuir* **2007**, *23*, 10499−10504.
(23) Zhu, Z. X.; Margulis-Goshen, K.; Magdassi, S.; Talmon, Y.; Macosko, C. W. Polyelectrolyte stabilized drug nanoparticles via flash nanoprecipitation: a model study with b-carotene. *J. Pharm. Sci.* **2010**, *99*, 4295−4306.
(24) Han, J.; Zhu, Z. X.; Qian, H.; Wohl, A. R.; Beaman, C. J.; Hoye, T. R.; Macosko, C. W. A simple confined impingement jets mixer for flash nanoprecipitation. *J. Pharm. Sci.* **2012**, *101*, 4018−23.
(25) Gindy, M. E.; Panagiotopoulos, A. Z.; Prud'homme, R. K. Composite block copolymer stabilized nanoparticles: simultaneous encapsulation of organic actives and inorganic nanostructures. *Langmuir* **2008**, *24*, 83−90.
(26) Zhu, Z. X. Polymer stabilized nanoparticles via flash nano-precipitation: particle formation, fomulation, and stability. Ph.D. Dissertation, University of Minnesota, Minneapolis, 2010.
(27) Zhu, Z. X. Effects of amphiphilic diblock copolymer on drug nanoparticle formation and stability. *Biomaterials* **2013**, *34*, 10238−48.
(28) Kumar, V.; Wang, L.; Riebe, M.; Tung, H. H.; Prud'homme, R. K. Formulation and stability of itraconazole and odanacatib nanoparticles: governing physical parameters. *Mol. Pharmaceutics* **2009**, *6*, 1118−1124.
(29) NCI Drug Dictionary. US National Cancer Institute; http://www.cancer.gov/drugdictionary (July 2013).
(30) Wohl, A. R. Synthesis and characterization of silicate ester prodrugs and poly(ethylene glycol)-b-poly(lactic-co-glycolic Acid) block copolymers for formulation into prodrug loaded nanoparticles. Ph.D. Dissertation, University of Minnesota, Minneapolis, 2012.
(31) Liu, Y.; Fox, R. O. CFD predictions for chemical processing in a confined impinging-jets reactor. *AIChE J.* **2006**, *52*, 731−744.
(32) Bird, R. B.; Stewart, W. E.; Lightfoot, E. N. *Transport phenomena*, 2nd ed.; Wiley International: New York, 2001.
(33) Macosko, C. W. *Rim: fundamentals of reaction injection molding*; Hanser Gardner Publications: Cincinnati, 1989.
(34) Mahajan, A. J.; Kirwan, D. J. Micromixing effects in a two-impinging-jets precipitator. *AIChE J.* **1996**, *42*, 1801−1814.
(35) Jakes, J. Testing of the constrained regularization method of inverting Laplace transform on simulated very wide quasielastic light-scattering auto-correlation functions. *Czech. J. Phys.* **1988**, *38*, 1305−1316.
(36) Jakes, J. Regularized positive exponential sum (REPES) program - a way of inverting laplace transform data obtained by dynamic light scattering. *Collect. Czech. Chem. Commun.* **1995**, *60*, 1781−1797.
(37) van Krevelen, D. W. *Properties of polymers*, 3rd ed.; Elsevier Science: New York, 1997.
(38) Hiemenz, P. C.; Rajagopalan, R. *Principles of colloid and surface chemistry*, 3rd ed.; Marcel Dekker Inc: New York, 1997.
(39) Lifshitz, I. M.; Slyozov, V. V. The kinetics of precipitation from supersaturated solid solutions. *J. Phys. Chem. Solids* **1961**, *19*, 35−50.
(40) Wagner, C. Theorie der Alterung von Niederschlagen durch Umlosen (Ostwald-Reifung). *Z. Elektrochem.* **1961**, *65*, 581−591.
(41) Hancock, B. C.; York, P.; Rowe, R. C. The use of solubility parameters in pharmaceutical dosage form design. *Int. J. Pharmaceutics* **1997**, *148*, 1−21.
(42) Kellogg, G. E.; Abraham, D. J. Hydrophobicity: is LogP(o/w) more than the sum of its parts? *Eur. J. Med. Chem.* **2000**, *35*, 651−661.
(43) Ali, H. S. M.; York, P.; Blagden, N.; Soltanpour, S.; Acree, W. E.; Jouyban, A. Solubility of budesonide, hydrocortisone, and prednisolone in ethanol + water mixtures at 298.2 K. *J. Chem. Eng. Data* **2010**, *55*, 578−582.
(44) Hagen, T. A.; Flynn, G. L. Solubility of hydrocortisone in organic and aqueous media: evidence for regular solution behavior in a polar solvents. *J. Pharm. Sci.* **1983**, *72*, 409−414.
(45) Saad, W. S. Drug nanoparticle formation via flash nano-precipitation: conjugation to encapsulate and control the release of paclitaxal. Ph.D. Dissertation, Princeton University, Princeton, 2007.
(46) Choi, P.; Kavassalis, T.; Rudin, A. Measurement of three-dimensional solubility parameters of nonyl phenol ethoxylates using inverse gas chromatography. *J. Colloid Interface Sci.* **1996**, *180*, 1−8.
(47) Marsac, P. J.; Shamblin, S. L.; Taylor, L. S. Theoretical and practical approaches for prediction of drug-polymer miscibility and solubility. *Pharm. Res.* **2006**, *23*, 2417−2426.
(48) Mordi, R. C.; Walton, J. C.; Burton, G. W.; Hughes, L.; Ingold, K. U.; Lindsay, D. A.; Moffatt, D. J. Oxidative degradation of beta-carotene and beta-apo-8′-carotenal. *Tetrahedron* **1993**, *49*, 911−928.
(49) Bhal, S. K.; Kassam, K.; Peirson, I. G.; Pearl, G. M. The rule of five revisited: Applying log D in place of log p in drug-likeness filters. *Mol. Pharmaceutics* **2007**, *4*, 556−560.

(50) Machatha, S. G.; Yalkowsky, S. H. Comparison of the octanol/water partition coefficients calculated by ClogP, ACDlogP and KowWin to experimentally determined values. *Int. J. Pharmaceutics* **2005**, *294*, 185−92.
(51) Pyka, A.; Babuska, M.; Zachariasz, M. A comparison of theoretical methods of calculation of partition coefficients for selected drugs. *Acta Pol. Pharm.* **2006**, *63*, 159−67.